THE OPTICAL POTENTIAL FOR MEDIUM-ENERGY PROTON SCATTERING

P. Schwandt, A. Nadasen,* P.P. Singh, M.D. Kaitchuck, W.W. Jacobs,
J. Meek, A.D. Bacher and P.T. Debevec**

The IUCF program of proton elastic cross-section measurements from nuclei at energies between 80 and 180 MeV is essentially completed. The previously reported[1] angular distributions for ^{28}Si, ^{40}Ca, ^{90}Zr and ^{208}Pb at several proton energies up to 160 MeV have recently been augmented by extension of the 135 MeV p + ^{90}Zr angular distribution to 126° and by measurements at 180 MeV for ^{90}Zr; an additional angular distribution for ^{208}Pb at 180 MeV is scheduled to be measured.

Together with the Maryland measurements[2] for ^{58}Ni, ^{90}Zr, ^{120}Sn and ^{208}Pb at 100 MeV, this new data set comprises 17 detailed and precise angular distributions, generally extending in angular range to 75-95° with angular intervals of 1-2°; relative errors are of order 3% and systematic errors do not exceed 10%. These measurements meet a need for high-quality proton elastic scattering data in this energy region which was only partially and inadequately met by older, less complete measurements at 155 MeV[3] and 185 MeV.[4]

The extension of our cross-section measurements beyond 90° (to angles where the cross section is of the order of several nb/sr) and to 180 MeV proton energy was made possible by a simple change from the usual spectrograph focal-plane detection system which consists of a 50 cm wide helical wire chamber followed closely by two equally wide plastic scintillators. Replacing the second wide scintillator with a narrow (10 cm) unit spaced 40 cm from the first scintillator reduced the coincidence background rate (largely from neutron-induced recoil protons) by nearly a factor of 50 to a level corresponding to ≃ 1nb/sr in cross section. The extended angular distribution obtained for ^{90}Zr at 135 MeV, spanning over 9 orders of magnitude in cross section, is illustrated in Fig. 1. The 180 MeV angular distribution for ^{90}Zr is shown in Fig. 2.

The IUCF data for ^{40}Ca, ^{90}Zr and ^{208}Pb were combined with existing ORNL data[5] at 61.4 MeV, Maryland data[2] at 100.4 MeV, and Uppsala data[4] at 181 MeV in a global analysis of proton elastic cross sections from these nuclei between 60 and 180 MeV. Using the IUCF automatic parameter search code SNOOPY6[6] the angular distributions were fit with a local, complex optical model potential

$$U(r) = U_{coul}(r) - Vf_o(r) - i\{W_s - 4a_w W_d \frac{d}{dr}\} f_w(r) + 2\{V_{so} + iW_{so}\}\frac{1}{r}\frac{d}{dr} f_{so}(r)\vec{L}\cdot\vec{\sigma}$$

with Woods-Saxon formfactors $f_i(r,r_i,a_i)$. The analysis was carried out in a semi-relativistic framework, i.e., using relativistic kinematics and a relativistic modification of the potential in the (intrinsically non-relativistic) Schrödinger equation following the Goldberger-Watson prescription.[7] The radial wave equation for the L^{th} partial wave retains the conventional non-relativistic form ($\hbar = c = 1$):

$$\{\frac{d^2}{d\rho^2} + (1 - \frac{\gamma V(\rho)}{T_c} - \frac{L(L+1)}{\rho^2})\} u_L(\rho) = 0$$

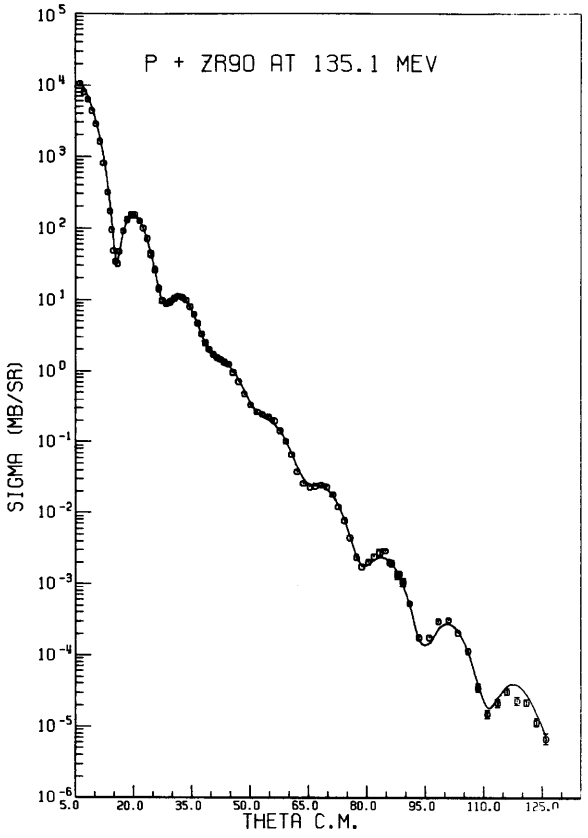

Figure 1

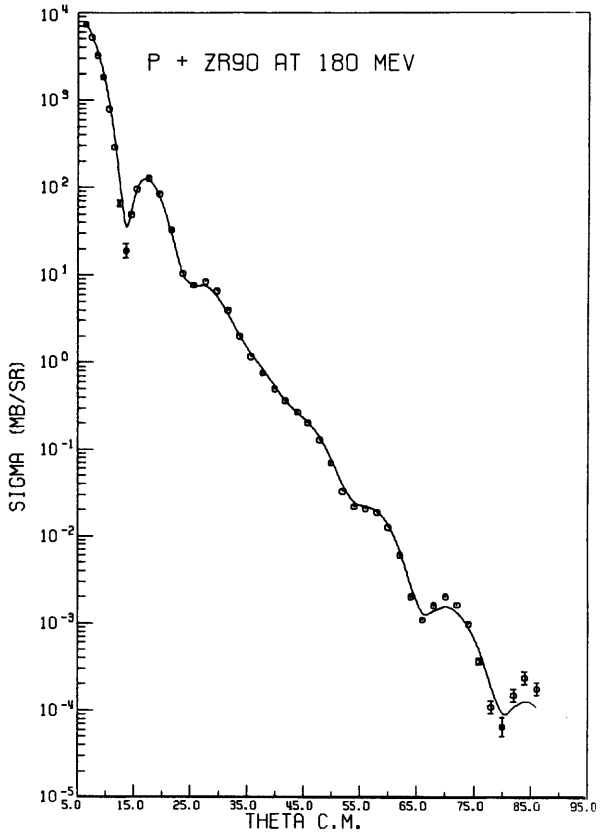

Figure 2

with $\rho = kr$, $k = \frac{m_2}{\sqrt{s}} \sqrt{T_{1L}(T_{1L} + 2m_1)}$, $T_c = T_{1c} + T_{2c}$, $\frac{\gamma}{T_c} \equiv \frac{2(\sqrt{s}-m_2)}{(\sqrt{s}-m_2)^2 - m_1^2}$ where $\sqrt{s} = T_c + m_1 + m_2$ denotes the total energy of projectile (1) and target nucleus (2) w.r.t. the center of mass. The relativistic correction factor γ multiplies <u>all</u> potential terms in this analysis even though no such simple relativistic modification of the spin-dependent term can be formulated. In particular, the Sommerfeld parameter $\eta = z_1 z_2 e^2 k/2T_c$ is also multiplied by γ, consistent with the corresponding correction to the Coulomb potential. Since this latter modification is found to have a relatively small effect on calculated observables (even for ^{208}Pb), the nuclear potential strengths reported here (in the form of γV etc.) may be used directly, to a good approximation, in a conventional non-relativistic optical-model or DW code <u>provided</u> relativistic kinematics are employed (i.e., if the relativistically correct values of k and T_c corresponding to projectile lab energy T_{1L} are entered into the program).

Although this type of relativistic approach is not strictly required to fit the present elastic scattering data (an equivalent but totally non-relativistic parametrization can be found), the use of relativistic kinematics, at the least, is deemed not only physically more realistic but advisable in view of the fact that distorted waves generated in the two approaches at these energies differ not

only in asymptotic phase (even in ρ-space) but can also differ markedly in radial dependence and magnitude in the nuclear surface and interior regions and hence can have sizeable effects on the results of reaction calculations in DWBA analyses (e.g., one finds nearly a factor 2 difference in a non-relativ. vs. relativ. calculation of the g.s. transition strength for the ^{40}Ca(d,p) reaction at 160 MeV, using optical potentials which give the same elastic scattering in each case).

Very satisfactory fits to the cross section data were obtained over the whole angular range when all 10 parameters V, r_o, a_o, W, r_w, a_w, V_{so}, W_{so}, r_{so}, a_{so} of the potential model were varied. The curves shown in Figs. 1 and 2 are representative of the general quality of fit. Constrained-geometry 6-parameter searches (with r_o, a_o, r_w, a_w fixed) also yielded subjectively good (and objectively acceptable) fits with reduced scatter of the associated strength parameters V, W as function of energy. These fixed-geometry parameters are tabulated in Table 1, along with corresponding volume integrals per nucleon, J_R/A and J_I/A, of the real and imaginary central potentials, the total reaction

Table 1. Fixed-Geometry Parameters

(r_o = 1.21, a_o = .77; r_w and a_w fixed at values indicated for each nucleus)

Target, Energy (MeV)	γV	γW_s	γW_d	(r_w)	(a_w)	γV_{so}	γW_{so}	r_{so}	a_{so}	$\frac{\gamma J_R}{A}$	$\frac{\gamma J_I}{A}$	$\frac{\sigma_R}{(mb)}$	$\frac{\chi^2}{N}$	γ	Data Ref.
^{28}Si 79.9	28.45	5.38	-	1.51	.42	2.90	-2.32	0.978	.495	303	84	399	26.2	1.039	pres.expt.
135.1	18.74	6.98	-	"	"	3.76	-1.69	1.031	.571	199	109	397	17.6	1.065	" "
^{40}Ca, 61.4	32.93	3.12	1.73	1.46	.48	4.06	-1.02	1.050	.616	328	71	575	2.1	1.031	5
80.2	30.74	7.16	-	"	"	3.38	-1.86	1.019	.489	306	102	615	10.5	1.040	pres.expt.
135.1	20.64	8.22	-	"	"	3.80	-0.76	1.088	.550	206	120	577	14.6	1.066	" "
160.0	19.10	8.01	-	"	"	3.54	-0.53	1.101	.567	190	114	534	18.0	1.077	" "
181	17.50	7.22	-	"	"	3.70	-0.56	1.096	.580	174	103	479	11.6	1.086	4
^{90}Zr, 61.4	36.19	4.67	1.82	1.41	.52	3.61	-1.80	1.106	.665	322	80	1122	4.1	1.031	5
79.8	33.20	6.80	-	"	"	2.41	-1.81	1.040	.476	295	85	1029	22.3	1.040	pres.expt.
100.4	28.93	7.05	-	"	"	2.91	-1.75	1.051	.536	257	88	977	3.4	1.050	2
135.1	24.60	9.55	-	"	"	3.37	-2.02	1.100	.572	219	120	1044	9.3	1.066	pres.expt.
160.0	24.50	7.87	-	"	"	3.34	-1.17	1.101	.592	218	98	922	15.8	1.078	" "
180	23.58	6.11	-	"	"	2.83	-0.71	1.109	.627	210	76	773	25.2	1.087	" "
^{208}Pb, 61.4	38.28	1.80	5.61	1.39	.57	5.84	-0.29	1.013	1.127	316	74	2000	2.4	1.032	5
79.9	31.92	9.42	-	"	"	4.67	-2.57	1.098	.581	264	111	1968	12.1	1.041	pres.expt.
100.4	32.18	6.37	-	"	"	4.23	-0.21	1.072	.778	266	75	1713	3.7	1.051	2
121.2	29.94	7.58	-	"	"	3.64	-1.27	1.092	.677	248	89	1756	6.7	1.060	pres.expt.
160.0	26.29	7.03	-	"	"	2.30	-0.80	1.129	.631	217	83	1618	14.4	1.078	" "
^{197}Au, 182	19.29	8.17	-	"	"	2.35	-1.88	1.131	.569	160	96	1567	19.6	1.088	4

(All potential strengths in MeV, geometry parameters in fm, volume integrals in MeV-fm^3)

Note that values of all potential strengths and volume integrals quoted here include the relativistic correction factor γ.

cross section σ_R, the quality-of-fit criterion χ^2/N per datum point, and the relativistic potential correction factor γ. Over the range of bombarding energies $60 \leq E \leq 160$ MeV and for target mass nos. $40 \leq A \leq 208$, the particular (E,A)-dependence found here (by no means unique) can be sufficiently well represented (for convenience of interpolation) by the relations

$$\gamma V = 91\ (1-.355 \log E) + 26\ \frac{N-Z}{A} \pm 1 \text{ MeV}$$

$$r_o = 1.21 \text{ fm}$$

$$a_o = 0.77 \text{ fm}$$

$$\gamma W_s \simeq 7.5 \pm 1.5 \text{ MeV} \quad (E \geq 80 \text{ MeV})$$

$$r_w = 1.37 + 3.5/A$$

$$a_w = 0.36 + .036\ A^{1/3}$$

The logarithmic energy dependence indicated here for the real central well depth is only approximately valid; results of analyses covering a wider energy range ($40 \leq E \leq 180$ MeV) indicate a reduction in the rate of fall-off of the real volume integral J_R with increasing energy. This deviation from the log E dependence indicated by the older, less complete data at 155 and 185 MeV is illustrated for ^{90}Zr in Fig. 3 (solid data and curve: present results; open circles and dashed line: previous data and trend).

No general systematic trend is perceived for the spin-orbit (S.O.) parameters, but the following characteristics are clearly established:

-- the S.O. radius parameter r_{so} is significantly smaller than the real central radius parameter r_o, generally increasing with energy from 1.03 to 1.13 fm.

-- an appreciable imaginary part to the S.O. potential (with $\overline{\gamma W_{so}} \simeq -1.4 \pm 0.5$ MeV) is definitely required at energies $E \geq 80$ MeV in order to reproduce the pronounced damping of the diffractive oscillations in the cross section universally observed in the mid-angle region 35-70° (that this damping is a direct manifestation of the S.O. interaction can be clearly demonstrated and has been previously reported[1]).

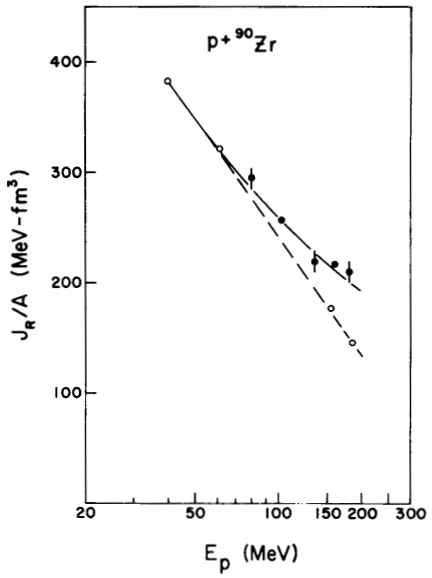

Figure 3

An imaginary component to the S.O. interaction of the sign and magnitude determined empirically in this analysis is entirely consistent with the expectation based on a simple impulse-approximation calculation of the first-order optical potential in terms of the free 2-nucleon forward-scattering amplitude which yields $\gamma V_{so} + i\gamma W_{so} \simeq 3.4 - 1.1i$ (MeV)

for 130-160 MeV proton scattering from ^{208}Pb, in embarrassingly good agreement with phenomenology (the validity of the impulse approximation for heavy nuclei at these energies is not all that good, even at low momentum transfer[8]).

The parametrization of the S.O. potential obtained by analyzing the new cross section data alone also provides a generally reasonable description of the existing polarization data[3,4,9] near 160 and 180 MeV. Although simultaneous fits to both cross sections and polarizations altered the S.O. parameters (as well as the central well parameters) somewhat, the changes are well within the range of parameter uncertainties and parameter correlations. Inclusion of the polarization data in the analysis did not help to reduce substantially the present S.O. parameter ambiguities, largely because of the relatively large experimental errors associated with the polarization data (± 0.03 to ± 0.15). Fig. 4 illustrates the variation in predicted polarization for ^{90}Zr at 135 MeV corresponding to a range of acceptable S.O. parameters (i.e., giving essentially equivalent cross sections). Significantly more accurate polarization measurements (to ± 0.02 - 0.05) must be made for a much better definition of the S.O. potential. Such measurements are planned to begin soon at IUCF (approved experiment # 66) utilizing the polarized proton beam from the IU polarized-ion source facility (cf. Section I). The insert in Fig. 4 shows, by means of contours of constant χ^2, the extent of the (V_{so},W_{so}) uncertainty and correlation, for example; the projected values indicate the ranges in V_{so},W_{so} for which the polarization predictions were made. The predominantly positive character of the polarization (becoming more pronounced with increasing energy) is another direct consequence of the imaginary S.O. term.

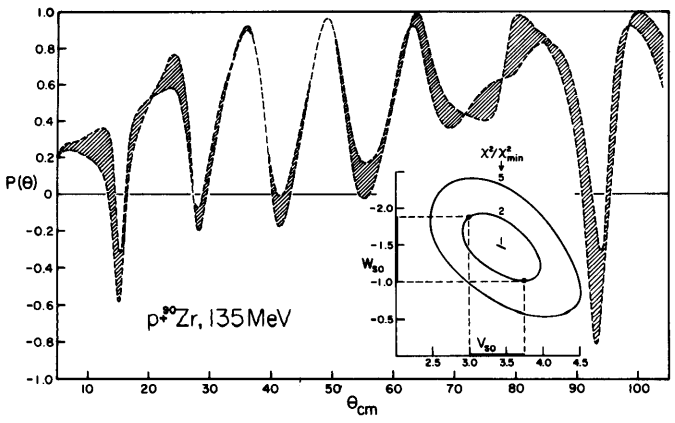

Figure 4

Significant correlations among various parameter pairs also exist for the central potentials. The potential volume integrals, largely independent of these parameter correlations, appear to be reasonably well defined by the present data; J_R is thought to be determined to ± 5% (with the main contribution to the uncertainty arising from the ± 10% cross-section normalization uncertainty). Parameter uncertainties are found to decrease steadily with increasing angular range of the data (typically by a factor 2-3 for θ_{max} between 60° and 120°). Deviation from the Woods-Saxon formfactor does not appear to be required by the data; relatively small changes in shape are tolerated by the

data through appropriate parameter readjustments. On the other hand, even small localized disturbances of the real central potential (notch perturbations) affect the fit significantly over a wide radial range (typically 2-7 fm); hence for proton scattering one does not find the kind of strong localization of the interaction (at any particular energy) one observes for more strongly absorbed projectiles.

A detailed report of this work is in preparation for publication.

Efforts are also underway to relate the principal features of the empirical optical-model potential (OMP) for proton-nucleus scattering obtained here to microscopically calculated OMP's based on realistic (strong) 2-nucleon interactions in multiple-scattering or Brueckner expansions.

*Present address: University of Maryland, Dept. of Physics, College Park, MD 20742

**Present address: University of Illinois Dept. of Physics, Urbana, IL 61801

1) IUCF Techn. and Scient. Report (Nov. 1975-Jan. 1977), pp. 45-48; A. Nadasen et al., BAPS 21, 978 (1976); ibid. BAPS 22, 543 (1977); A. Nadasen, Ph.D. thesis (Indiana Univ. 1977); P. Schwandt, Intern. Symposium on Nucl. Phys. at Cyclotron Energies, Calcutta (India), Sept. 1977 (unpublished).

2) K. Kwiatkowski, Ph.D. thesis (Univ. of Maryland 1976); K. Kwiatkowski and N.S. Wall, Univ. of Maryland Report PP 78-062.

3) A. Willis et al., Nucl. Phys. A112, 417 (1968); V. Comparat et al., Nucl. Phys. A221, 403 (1974).

4) A. Johansson et al., Arkiv f. Fysik 19, 541 (1961); A. Ingemarsson and G. Tibell, Physica Scripta 4, 235 (1971); E. Hagberg et al., Physica Scripta 3, 245 (1971).

5) C.B. Fulmer et al., Phys. Rev. 181, 1565 (1969).

6) P. Schwandt, IUCF Intern. Report # 77-8.

7) Goldberger and Watson, Collision Theory (Wiley, New York 1964).

8) V. Comparat, Ph.D. thesis (Univ. of Paris/ Orsay 1975).

9) A. Willis et al., Journ. Physique 30, 13 (1968).